Matured Theobroma Cocoa Pod Extracts as Green Inhibitor for Acid Corrosion of Aluminium

Shwethambika, P.•; Ishwara Bhat J.*+

Department of Chemistry, Mangalore University, Mangalagangotri-574199, Karnataka, INDIA

ABSTRACT: *Matured Cocoa Pod Extract (MCPE) is prepared using Soxhlet extraction and is then characterized using Fourier Transform-Infra Red Spectroscopy (FT-IR), Gas Chromatography-Mass Spectroscopy (GC-MS). The thermal decomposition characteristics are studied using Thermo Gravimetric Analysis- Differential Thermal Analysis (TGA-DTA) method. FT-IR study confirmed the presence of hetero atoms like O, N and GC-MS showed the presence of 15 chemical constituents of which 1,2-bis (trimethylsilyl) benzene is the major constituent present. TGA-DTA studies showed the thermal decomposition of chemical constituents which was supported by GC-MS data. The inhibition efficiency of MCPE is tested in 0.5M HCl medium taking aluminium as target metal by Weight loss method (303K-308K). Anticorrosive property of MCPE was also tested using Electrochemical Impedance Spectroscopy and Potentiodynamic Polarization methods (303K). In all the methods, the inhibition efficiency of MCPE found to increase with increase in % volume of the MCPE exhibiting good agreement with each other. Also, inhibition efficiency decreased with increase in temperature, showing adsorption of inhibitor is by physisorption and thermodynamic parameters are measured. Tafel plots showed MCPE could retard both anodic and cathodic reactions, predominantly acting as anodic type of inhibitor. Surface morphological changes of the metal were studied using Scanning Electron Microscopy which confirmed that MCPE acted as inhibitor by adsorption mechanism.*

KEYWORDS: *Acid corrosion; Aluminium; Cocoa pod extract; EIS; Green inhibitor; Tafel method; Weight loss.*

INTRODUCTION

Corrosion is a phenomenon related to the degradation of material due to the interaction between the material and the environment. The metal gets converted to its stable form by undergoing oxidation either to its oxide, carbonate or hydroxide form due to the corrosion reaction which leads to the loss of precious metal takes place thus leading to the enormous economic loss in industries and everyday life [1]. Aluminium is one of the important and very abundant metal on earth crust and possess low density, non-toxic, high thermal conductivity and is known to be a good electrical conductor. Aluminium finds wide applications in domestic as well as industrial sectors. So the metal frequently comes in contact with aggressive medium and or acid solutions which lead to the corrosion of aluminium [2, 3].

Use of corrosion inhibitors is an important method to control the problem of corrosion. Among the known

** To whom correspondence should be addressed.*

+ E-mail: bhatij08@gmail.com

● *Other Address: Department of Chemistry, Vivekananda College of Engineering and Technology, Puttur-574203, Karnataka, INDIA*

1021-9986/2021/3/906-919 14/$/6.04

Fig. 1: Theobroma cocoa fruit.

Fig. 1: Theobroma cocoa fruit.

methods literature survey shows that inhibitors possess hetero atoms like O, N and S which get adsorb on to the surface of the material and block the active sites, thereby reducing the rate of corrosion [9-18]. However, the literature study shows that the synthetic inhibitors are quite harmful for environment and living kind due to its toxicity. So use of inhibitors originated from plant, called as green inhibitors find its prime importance in the field of corrosion control. They are found to be environmentally safe, biodegradable, relatively cheap, and non-harmful [19-22].

Theobroma Cocoa. L, plant yields edible fruit and grown in India. The fruit of Cocoa plant possess beans which are dried and used in food industries for the production of chocolates and confectioneries [23]. The images of *Theobroma Cocoa* fruit and Matured Pod images are shown in Fig.1 and Fig. 2. [24, 25] *Azizah Othman et.al,* have studied the antioxidant capacity and phenolic content of cocoa beans. The studies reveal that cocoa is a rich source of phenolic compounds [26]. *L.E. Umoru et.al,* have studied the inhibitive influence of *Theobroma Cacao* and C*ola Acuminata Leaves* extracts prepared by contact extraction with methanol on the corrosion of a mild steel in sea water by weight loss method[27]. *Yuli Yetri Emriadi et al.,* have studied corrosion inhibitor of mild steel by polar extract of *Theobroma cacao* peels in hydrochloric acid solution by weight loss and potentiodynamic polarization methods [28].

Thus in the present work, the pod of Asian matured Cocoa fruit, which is discarded as an agricultural waste after the use of its beans, is collected from local agriculturists of Southern Karnataka, India. This is then extracted with methanol by Soxhlet extraction unit and characterized using different spectroscopic methods namely FT-IR and GC-MS methods. Thermal stability and decomposition characteristics of the extract are studied using TGA-DTA method. The obtained extract is investigated for its corrosion inhibitive properties for aluminium in 0.5M HCl using Weight loss, Electrochemical Impedance Spectroscopy (EIS) and Potentiodynamic Polarization methods. Surface morphological changes of the target metal are studied using Scanning Electron Microscopy (SEM) technique.

EXPERIMENTAL SECTION

Preparation of the Matured Cocoa Pod Extract (MCPE)

Matured *Theobroma cocoa* pod sample was collected from Cocoa growers. The sample was cleaned from dirt with double distilled water, was finely cut into pieces, and extracted with methanol using Soxhlet extraction apparatus for about 6 hours. The extract was filtered through Whatman no.1 filter paper. The obtained *Matured Cocoa Pod* Extract (MCPE) was a yellow coloured liquid. Different volumes of MCPE were taken for corrosion inhibition test viz., 8%, 16%, 24% and 32% by volume of the aggressive medium.

Characterization of MCPE

Fourier Transform-Infra Red (FT-IR) spectroscopy

About 10 mg of liquid MCPE sample was used for recording the FT-IR using Perkin Elmer - Spectrum RX-IFTIR instrument. Spectrum was recorded with a resolution of 1 cm^{-1} and in the scan range of 4000 cm^{-1} to 250 cm^{-1}. It was then used for the identification of different functional groups most likely to be present in the MCPE.

Gas Chromatography-Mass Spectroscopy (GC-MS)

The GC-MS analysis of the sample was performed using a Shimadzu GCMS-QP2010 gas chromatography mass spectrometer interfaced with a Turbo Mass

quadrupole spectrometer using helium as carrier gas. The mass spectra were taken with a mass scan range of 40-600Da. The spectrum obtained was used to get information about the chemical constituents [6] by comparing it with the data provided in National Institute of standards and Technology (NIST) library.

Thermo Gravimetric analysis- Differential Thermal analysis (TGA-DTA)

The MCPE sample was examined for its thermal stability of using *TGA- DTA* technique. The spectrum was recorded using instrument SDT Q600 V20.9 Build 20. The MCPE was evaporated in the presence of methanol and the residue obtained was in gel form. About 6-10mg of residue sample was subjected to thermal decomposition in alumina pan using Nitrogen gas. The data provided was used to study the thermal decomposition characteristics of the chemical constituents present in MCPE [7, 8].

Weight loss studies

Preparation of metal samples

Aluminium Al-63400 (equivalent alloy U.S.A- AA 6063) subjected to undergo weight-loss measurements. The composition of the target metal is shown in Table 1 [29-31].

The metal sample was cut into identical size of 1.5 inch*1.5 each, well cleaned with water and polished with different emery papers ranging from 80 to 2000 grade, cleaned with acetone, washed with double distilled water, and dried well and was used for weight loss measurements.

Preparation of corrosion medium

Corrosive medium of 0.5 M HCl was prepared by diluting SDFCL analytical grade 35-38% HCl using double distilled water.

Weight loss measurements

Initially surface prepared the aluminium metal samples were weighed and then suspended in 60mL of corrosive medium (0.5M HCl) in the absence and presence of different volumes of MCPE at 303K.. After 5 hours, the aluminium samples were taken out from the corrosive medium, washed with double distilled water, dried and weighed accurately. Then the rate of corrosion (*CR*) of aluminium was determined using Eq. (1) [29, 30].

$$CR = \frac{534 \times W}{A \times T \times D} \quad (1)$$

Where *CR* is the corrosion rate of aluminium in mils penetration/year (mpy), *W* is the weight loss of aluminium (in mgs), *A* is the area of metal sample (in square inches), *T* is the time of exposure (in hours) and *D* is the density of aluminium (in grams/cubic centimeter). The inhibition efficiency is calculated using Eq. (2) [32, 33]

$$\text{Inhibition Efficiency} = \frac{W_2 - W_1}{W_2} \times 100 \quad (2)$$

Where W_1 and W_2 are weight loss of aluminium samples in the presence and absence of the inhibitor MCPE respectively.

Effect of temperature

To study the effect of temperatures on inhibition efficiency of MCPE, the weight loss studies were carried out at 308, 313, 318 and 323K. The corrosion rate and inhibition efficiency were calculated as per Eq. (1) and Eq. (2) respectively.

Electrochemical Impedance Spectroscopy (EIS) and potentiodynamic polarization method:

EIS study was carried out using aluminium as target metal with approximately a circular area of $1cm^2$ exposed to corrosive environment. Rest of the sample area was covered with acrylic repair material. Before the use, the test materials were well cleaned and polished with different emery papers ranging from 80 to 2000 grade. They were applied with machine polish using alumina water and then washed thoroughly with water, cleaned with acetone, washed with double distilled water and dried well for further study.

Electrochemical measurements were recorded using a GillAc Potentiostat CH 1480 analyser at 303K by taking aluminium as working electrode. Saturated calomel electrode (SCE) was connected as reference electrode, and platinum electrode as auxiliary electrode. All AC impedance measurements were taken using an AC signal with amplitude of 10*mV* at Optimum Cell Potential (OCP) in the frequency range from 0.01*Hz* to 1M *Hz*. The Potentiodynamic Polarization studies were also carried out similarly and potential–current curves (Tafel plots) were recorded by polarizing the specimen to -250 mV to +250 mV against OCP at scan rate of 1mV/s.

Table 1: Chemical composition of Al-63400.

Element	Cu	Mg	Si	Fe	Mn	Zn	Cr	Tl	Al
Weight%	0.1	0.4−0.9	0.3−0.7	0.6	0.3	0.2	0.2	0.1	Remainder (96.9−97.8%)

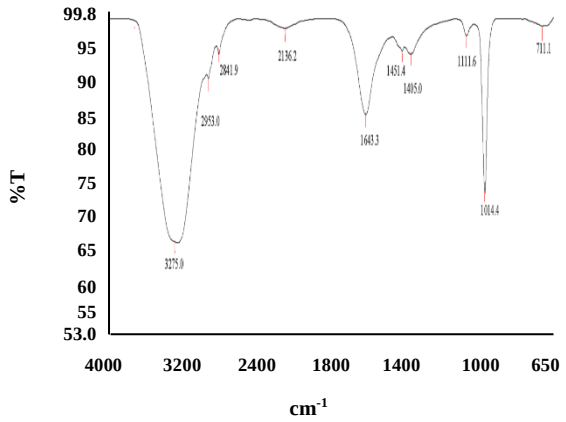

Fig. 3: FT-IR Spectrum of MCPE.

Scanning Electron Microscopy

Surface morphology of the aluminium metal samples was examined by Carl Zeiss field emission scanning electron microscope (FESEM) [21]. The surface prepared metal samples were exposed to corrosive environment for 5 hours in the absence and presence of optimum concentration of the MCPE inhibitor in 0.5M HCl at 303K. The surface images of the samples were then recorded using scanning electron microscope immediately after the corrosion test.

RESULTS AND DISCUSSION:

Fourier Transform-Infra Red (FT-IR) spectroscopy

The FT-IR spectrum of MCPE is shown in Fig. 3. The analysis gave information about the presence of different functional groups in the MCPE sample.

A broad peak at 3275cm^{-1} shows the presence of -OH group [4]. Also a sharp peak is shown at 1643cm^{-1} corresponds to the presence of C=O stretch for amides [5]. A sharp peak of C-O stretch from esters is also found in the range from 1300-1000cm^{-1}[34, 35]. Details about the probable functional groups that likely to be exist in MCPE with the corresponding wave numbers are listed in Table 2 [4, 5 and 36]

Gas chromatography-Mass Spectroscopy (GC-MS)

From the GC-MS spectrum obtained, for a given retention time, the peaks corresponding to different m/z (mass to charge number of ion) values are compared with the literature and about 15 possible constituents are identified and listed in Table 3 [37-38]. The extract showed maximum peak area of 24.515% with retention time of 26.718. The GCMS peak obtained for retention time 26.718 is shown in Fig. 4. The peak corresponds to the presence of chemical constituent 1, 2-bis (trimethylsilyl) benzene, so this chemical can be considered as the major constituent in the extract and structure of the compound is shown in Fig.5.

Thermo gravimetric Analysis of MCPE:

The spectrum obtained from the TGA-DTA is shown in Fig.6. The study of the graph showed the presence of 4 major peak regions and a horizontal region at different temperatures namely Region 1: 30-150^{0}C, Region 2: 150-250^{0}C, Region 3: 250-350^{0}C, Region 4: 600-650^{0}C and Region 5: 675-700^{0}C.

In Region 1, the evaporation of moisture and volatile contents of MCPE is found along with some low melting chemical constituents [39]. Comparing the TGA data with GCMS data, the chemical constituents which have undergone thermal decomposition in those peaks region, present in the extract were identified and are listed in Table 4. Region 5: 675-700^{0}C shows no much variations (almost horizontal) corresponding to the presence of metals present in the MCPE [40].

Correlation of FT-IR, GC-MS and TGA-DTA study

The results obtained from FT-IR showed the presence of different functional groups and presence of O, N and Si in the MCPE inhibitor. GC-MS data showed the major constituent present in MCPE with other existing chemical constituents. The functional groups present in those chemical constituents were also identified in FT-IR results, mutually supporting each other. TGA-DTA studies showed the decomposition of MCPE at different temperature range and GC-MS data obtained supported the same. Also major % weight loss was shown in the temperature range near 100^{0}C-120^0 C which supported

Table 2: List of functional groups and their stretching frequencies on FT-IR analysis for MCPE.

Wave Numbers (cm^{-1})	Corresponding identified functional group in MCPE
3275	Stretching vibration of –O–H groups [3400-3200] /–NH stretch of amines [3500-3300]
2953,2841	C-H stretch for sp^3 hybridized carbon of methyl group [3000-2840]
2136	C-H stretching vibrations of alkynes[2200-2040]
1643	C=O Stretch for amides [1695-1630]
1451	C=C stretch, aromatic HC chromophore [1500-1450]
1405	=C-H bending for substituted alkenes [1420-1410]
1111	Si–C_6H_5 bond from substituted ring structure[1130-1110]
1014	Si-CH_3 stretches for alkyl silanes[1100-950]/ C-O stretch from esters [1300-1000]
719.5	C-H out-of-plane bending [685-715]

Table 3: List of compounds identified in MCPE by GC-MS.

Sl. No.	Chemical Constituents identified	Retention Time (min)	Molecular Formula	Molecular Mass
1	1,2-Ethanediol, Mono Acetate	3.929	$C_{12}H_8O_3$	104
2	3-Amino-2-Oxazolidinone	10.221	$C_3H_6O_2N_2$	102
3	DL-Cystathionine	18.395	$C_{17}H_{24}O_4N_2S$	222
4	Bicyclo[2.2.1]Heptan-2-One,4,7,7-Trimethyl-Semicarbazone	19.655	$C_{11}H_{19}ON_3$	209
5	Undecanoic Acid, 11-Flouro-Trimethyl Silyl Ester	19.970	$C_{14}H_{29}O_2FSi$	276
6	Silicic Acid, Diethyl Bis (Trimethyl Silyl) Ester	25.878	$C_{10}H_{28}O_4Si_3$	296
7	1,4-Cyclohexadiene, 1,3,6-Tris(Timethylsilyl)	25.898	$C_{15}H_{32}Si_3$	296
8	1-Penta Methyl Disilyloxy Tridecane	26.158	$C_{18}H_{42}OSi_2$	330
9	1,3-Bis-T-Butylperoxy-Phthalan	26.283	$C_{16}H_{24}O_5$	296
10	N-Methyl-1-Adamantaneacetamide	26.383	$C_{13}H_{21}ON$	207
11	1-Monolinoleoylglycerol Trimethylsilyl Ether	26.518	$C_{27}H_{54}O_4Si_2$	498
12	1,2-Bis(Trimethylsilyl)Benzene	26.718	$C_{12}H_{22}Si_2$	222
13	Trimethyl(4-Tert.-Butylphenoxy)Silane	26.913	$C_{13}H_{22}OSi$	222
14	Acetic Acid, 3-Hydroxy-7-Isopropenyl-1,4a-Dimethyl-2,3,4,4a,5,6,7,8-Octa	30.710	$C_{17}H_{26}O_3$	278
15	Benzene, 2-[(Tert-Butyldimethylsilyl)Oxy]-1-Isopropyl-4-Methyl	31.210	$C_{16}H_{28}OSi$	264

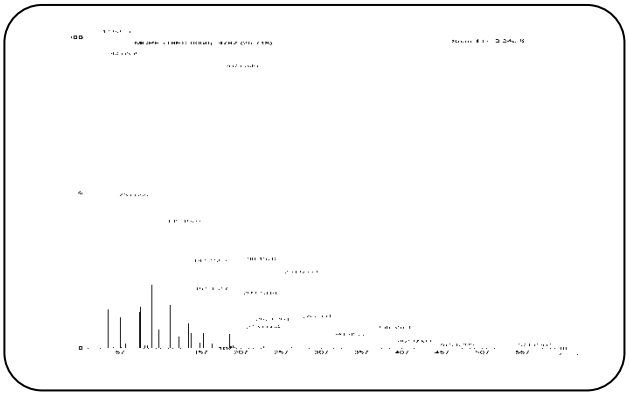

Fig. 4: GCMS peaks for R_t=26.718.

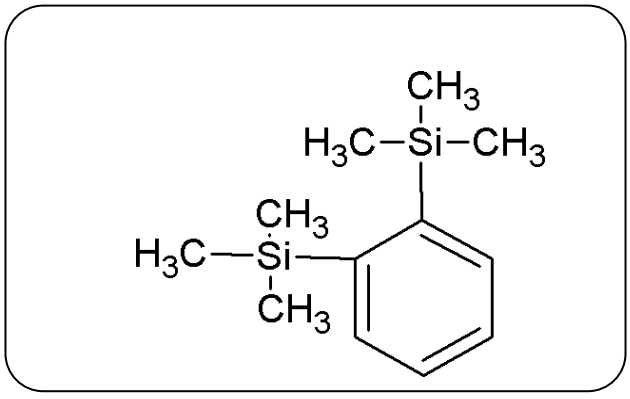

Fig. 5: 1, 2-bis (trimethylsilyl) benzene.

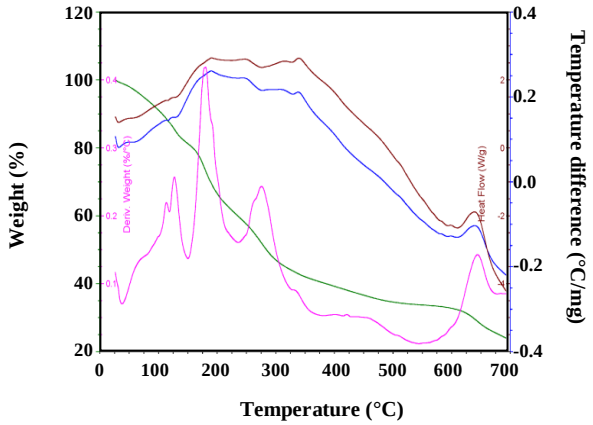

Fig. 6: TGA-DTA spectrum of MCPE.

GC-MS data interpretation i.e., 1,2 (bistrimethyl) silyl benzene as the major chemical constituent of MCPE.

Weight loss measurements

Weight loss studies for aluminium in 0.5M HCl in the absence and presence of MCPE showed that, with the increase in % volume of MCPE, there is a decrease in the corrosion rate and increase in the inhibition efficiency. It was found that a maximum inhibition efficiency of 84.81±1.77% was obtained and there afterwards it remained almost constant. The data obtained from the weight loss measurements are tabulated in the Table 5.

Effect of temperature

The study of effect of temperature showed that, with the increase in temperature, there is an increase in corrosion rate and decrease in inhibition efficiency of MCPE. This trend may be attributed due to desorption of adsorbed organic molecules from MCPE at elevated temperatures [41, 42]. The weight loss data obtained for aluminium in 0.5M HCl at various temperatures are listed in Table 6. The corrosion rate variation with % volume of MCPE at different temperatures is shown in Fig. 7. From the Fig. 7 it is clear that, with the increase in temperature of reaction medium, the corrosion rate of the aluminium shows a considerable increase indicating there is decrease of inhibition efficiency of MCPE.

The apparent activation energy of metal corrosion in acid media was calculated from the Arrhenius equation shown as Eq. (3) [43, 44]

$$\ln(\text{Corrosion rate}) = \ln A - \frac{Ea^0}{RT} \qquad (3)$$

Where $E_a{}^0$ is the apparent activation energy for the corrosion of aluminium , R is the universal gas constant, A is Arrhenius pre exponential factor and T is the absolute temperature. The plot of ln(*Corrosion Rate*) *vs. 1000/T* is shown in Fig. 8 and the values of $E_a{}^0$ obtained from the slope of the plot. The obtained values are tabulated in Table 7.

It is observed that, also with the increase in % volume of MCPE, the $E_a{}^0$ values show an increase, which can be due to the adsorption of the inhibitor on the aluminium surface thus forming a barrier at metal-solution interface which limits the contact of metal with corrosive medium [45]. *Ekanem U. F., Umoren S. A. et.al*, explained that with the increase in temperature, an appreciable decrease in the adsorption of the inhibitor on the metal surface takes place, showing the increase in activation energy. This exposes greater area of metal to the acid environment and causes a corresponding increase in corrosion rate [46].

An alternative form of Arrhenius equation is the transition state equation as Eq. (4) [45, 46]

$$\text{Corrosion rate}(CR) = \frac{RT}{Nh}\exp\left(\frac{\Delta Sa^0}{R}\right)\exp\left(-\frac{\Delta Ha^0}{RT}\right) \qquad (4)$$

where, h is the Plank's constant, N is the Avogadro's number, $\Delta S_a°$ is the entropy of activation, and ΔH_a ° is the enthalpy of activation. A plot of *ln (CR/T) vs. 1/T* is shown in Fig. 9. The slope of lines obtained is given by ($-\Delta H_a°/R$) and intercept by [$ln(R/Nh) + (\Delta S_a °/R)$], from which the values of ΔH_a ° and ΔS_a ° were calculated and listed in Table 7.

The values of $\Delta H_a°$ obtained are positive both in the presence and absence of the inhibitor shows that, the metal dissolution process is endothermic type for the corrosion of aluminium in HCl medium. It is also shown that with the increase in the % volume of the MCPE there is increase in $\Delta S_a°$ values. This increase in entropy from uninhibited corrosion medium to inhibited corrosion medium suggesting that there is an increase in the randomness occurred while moving from reactants sate to the activated complex state [47, 48].

Electrochemical Impedance Spectroscopy (EIS)

The data obtained from EIS study showed a decrease in corrosion rate with increase in % volume of MCPE thus supporting the data obtained through weight loss measurements. The impedance spectra contain depressed

Table 4: List of compounds in MCPE grouped according to their melting point and boiling point.

Sl.No.	Decomposition Region	Chemical Constituents identified	Melting point (^{0}C)	Boiling point (^{0}C)
1	30-150^{0}C	Undecanoic Acid, 11-Flouro-Trimethyl Silyl Ester	38.18	-
		1,2-Ethane-Diol, Mono Acetate	45.54	-
		1-Penta Methyl Disilyloxy Tridecane	47.4	-
		Trimethyl(4-Tert.-Butylphenoxy)Silane	54-58	-
		Benzene, 2-[(Tert Butyl dimethyl silyl)Oxy]-1-Isopropyl-4-Methyl	66.98	-
		1,3-Bis-T-Butylperoxy-Phthalan	106.47	-
		1,2-Bis(Trimethylsilyl)Benzene		115
		Bicyclo[2.2.1]Heptan-2-One,4,7,7-Trimethyl-Semicarbazone	117.77	-
		Acetic Acid, 3-Hydroxy-7-Isopropenyl-1,4a-Dimethyl-2,3,4,4a,5,6,7,8-Octa	123.52	-
		N-Methyl-1-Adamantaneacetamide	128.4	-
		3-Amino-2-Oxazolidinone	137	-
2	150-250^{0}C	1-Monolinoleoylglycerol Trimethylsilyl Ether	168.1	-
		Silicic Acid, Diethyl Bis (Trimethyl Silyl) Ester	-	225.88
		1,2-Ethane-Diol, Mono Acetate	-	240.50
		1,4-Cyclohexadiene, 1,3,6-Tris(Timethylsilyl)	-	247.26
3	250-350^{0}C	3-Amino-2-Oxazolidinone	-	281.12
		Trimethyl(4-Tert.-Butylphenoxy)Silane	-	282.04
		Undecanoic Acid, 11-Flouro-Trimethyl Silyl Ester	-	295.9
		Benzene, 2-[(Tert Butyl dimethyl silyl)Oxy]-1-Isopropyl-4-Methyl	-	311.2
		DL-Cystathionine	315-316	-
		1-Penta Methyl Disilyloxy Tridecane	-	316.4
		Bicyclo[2.2.1]Heptan-2-One,4,7,7-Trimethyl-Semicarbazone	-	333.54
		N-Methyl-1-Adamantaneacetamide	-	346.9
		1,3-Bis-T-Butylperoxy-Phthalan	-	349.2
		Acetic Acid, 3-Hydroxy-7-Isopropenyl-1,4a-Dimethyl-2,3,4,4a,5,6,7,8-Octa	-	351.95

Table 5: Inhibition efficiency of MCPE by weight loss studies for aluminium in 0.5M HCl at 303K.

% Volume	Weight loss (g)	Corrosion Rate (mpy)	Inhibition efficiency (%)
0	0.0079	104.51	
8	0.0057	75.41	27.84±0.97
16	0.0036	47.62	54.43±1.86
24	0.0025	33.07	68.35±1.41
32	0.0012	15.87	84.81±1.77
40	0.0013	17.19	83.54±1.52

Table 6: Weight loss data of aluminium in 0.5M HCl in the presence and absence of MCPE (308-323K).

Temperature (K)	% Volume	Weight loss (g)	Corrosion Rate (mpy)	Inhibition efficiency (%)
308	0	0.0150	198.01	-
	8	0.0116	153.02	22.72
	16	0.0077	101.43	48.78
	24	0.0057	74.97	62.14
	32	0.0036	47.62	75.95
	40	0.0036	47.62	75.95
313	0	0.0227	299.88	-
	8	0.0186	246.51	17.79
	16	0.0134	177.28	40.88
	24	0.0107	141.12	52.94
	32	0.0069	91.72	69.41
	40	0.0070	93.04	69.16
318	0	0.0308	407.92	-
	8	0.0275	364.26	10.70
	16	0.0211	279.15	31.57
	24	0.0174	230.20	43.57
	32	0.0126	166.69	59.14
	40	0.0127	168.01	58.76
323	0	0.0429	568.01	-
	8	0.0395	523.02	7.92
	16	0.0314	415.86	26.79
	24	0.0269	355.44	37.42
	32	0.0196	259.74	54.27
	40	0.0196	259.74	54.27

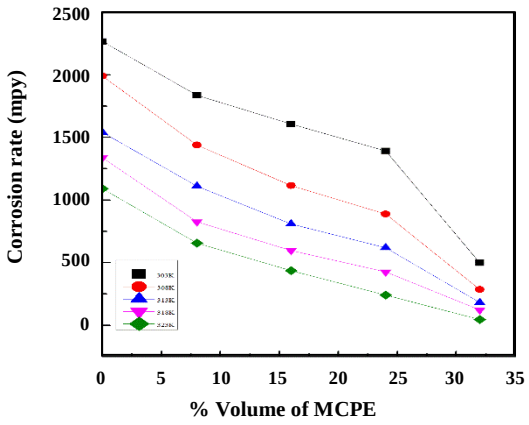

Fig. 7: Variation of corrosion rate of aluminium in 0.5M HCl with different % volume of MCPE at different temperatures.

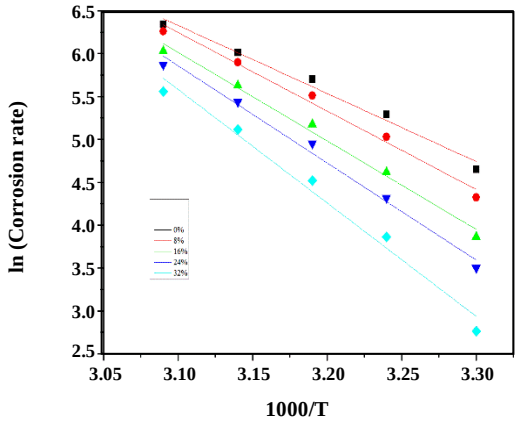

Fig. 8: ln(Corrosion Rate) vs. 1000/T for aluminium in 0.5M HCl.

Table 7: Activation parameter values for aluminium in 0.5M HCl.

% Volume of MCPE	Energy of activation E_a (kJmol^{-1})	Arrhenius Factor (A*10^{13})	Enthalpy ΔH_a^0 (kJmol^{-1})	Entropy ΔS_a^0(Jmol^{-1}/K)
0	65.98	2.71	63.18	114.58
8	76.09	1.07*10^2	73.29	145.26
16	85.72	3.12*10^3	82.95	173.26
24	94.11	6.21*10^4	91.37	198.05
32	109.91	1.68*10^7	107.15	244.69

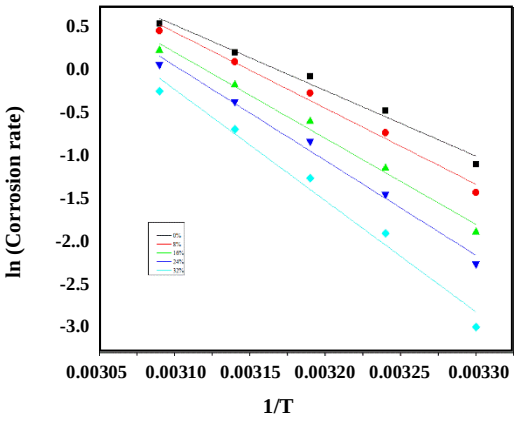

Fig. 9: ln(Corrosion Rate/T) vs. 1/T for aluminium in 0.5M HCl.

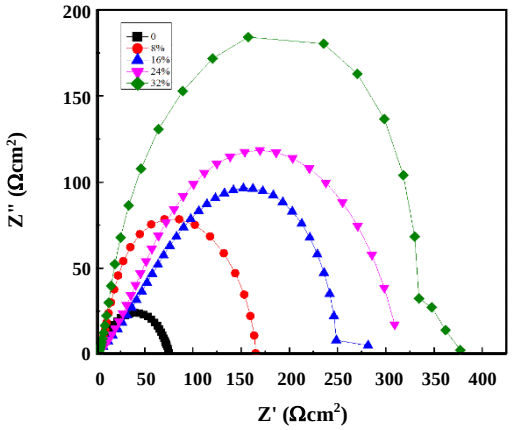

Fig. 10: Nyquist plot for aluminium in 0.5M HCl with various % volumes of MCPE at 303K.

semicircle with centre under real axis known as Nyquist plot shown in Fig.10 at 303K. The values of resistance due to charge transfer (R_{ct}) and frequency for maximum Z'' (ω_{max}) was obtained using software ZsimpWin Version 3.21 by circle fitment. A good fit between calculated and measured Z data is observed. The fitted graph is shown in Fig.11 (a) and the equivalent circuit is shown in Fig 11 (b).

From the Fig. 10, it is seen that size of semicircle increased with increase in % volume of MCPE. It also shows that the impedance of solution increased with the increase in % volume of MCPE. The resistance due to charge transfer (R_{ct}) also showed an increase with % volume of MCPE. This may be attributed due to decrease in local dielectric constant and/or increase in thickness of the electrical double layer [47].The inhibition efficiency of the MCPE inhibitor is given by Eq. (5) [48].

$$\text{Inhibition efficiency I.E.}(\%) = \left[\frac{(Rct_{inh} - Rct)}{Rct_{inh}}\right] \times 100 \quad (5)$$

Where Rct is resistance due to charge transfer without inhibitor, and $Rct_{(inhi)}$ is resistance due to charge transfer with inhibitor. Capacitance of double layer (C_{dl}) value is obtained from the Eq. (6) [49]

$$C_{dl} = \frac{1}{R_{ct} \times \omega_{max}} \quad (6)$$

where, ω_{max} is the frequency at the top of the semicircle. (where-Z'' is maximum).The data obtained by the experimental result of EIS measurements for the corrosion of aluminium in 0.5 M HCl in the absence and presence of MCPE is given in Table 8.

From Table 8, it is also shown that the capacitance of double layer (C_{dl}) got decreased with increase in % volume of MCPE. This might be caused due the replacement of water molecules by the adsorbed organic molecules from MCPE and thereby decreasing the rate of metal dissolution in acid medium [47-50].

Polarization studies

Potentiodynamic Polarization curves for aluminium sample in 0.5 M hydrochloric acid recorded in the absence and presence of different concentration of the MCPE inhibitor are shown in Fig. 12.

Table 8: AC impedance data of aluminium in 0.5 M HCl solution at 303K for various % volumes of MCPE.

% Volume of MCPE	R_{CT}	I.E (%)	C_{dl} (μ F)
0	75	-	103
8	141	47.07	21.2
16	239	69.03	17.0
24	343	76.72	12.8
32	400	81.18	10.3

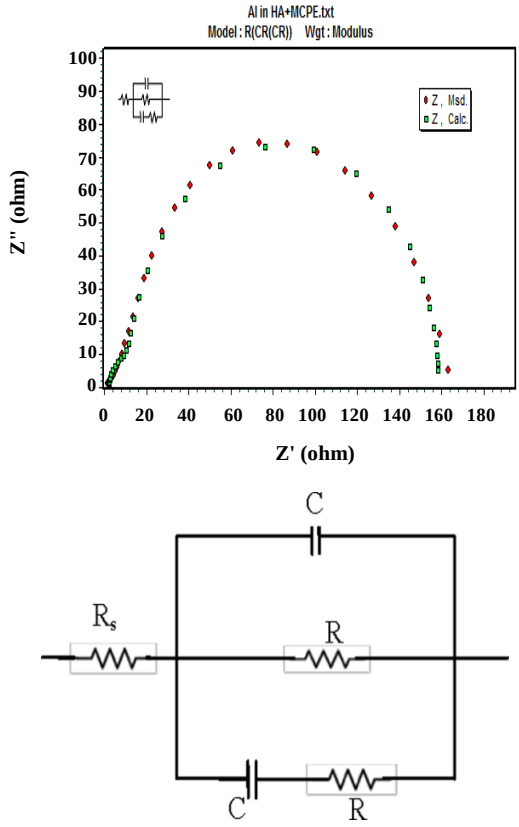

Fig. 11: (a) Circuit fitment for the EIS measurements for aluminium in HCl with 8% MCPE, (b) Equivalent circuit for aluminium in HCl with 8% MCPE.

The electrochemical parameter values, such as corrosion current densities (i_{corr}), Tafel anodic slopes (βa), Tafel cathodic slopes (βc), Corrosion rate, inhibition efficiency (*%IE*) and corrosion potential (E_{corr}) calculated are listed in Table 9. The inhibition efficiency is given by Eq. (7) [50].

$$\text{Inhibition efficiency}(\%) = \left[1 - \left(\frac{i'corr}{icorr}\right)\right] \times 100 \qquad (7)$$

Where, i'_{corr} and i_{corr} are the corrosion currents in the presence and absence of the MCPE inhibitor respectively.

From the values listed in Table 9, it is clear that the values of inhibition efficiency got increased and corrosion current got decreased with the increase in % volume of MCPE showing that MCPE acted as a good inhibitor for corrosion of aluminium in 0.5 M HCl. Also decrease in both anodic and cathodic slopes showed that MCPE is retarding both cathodic and anodic reactions [51]. Further amongst βa and βc, since βa showed a large decrease in its vales, inhibitor can be expected to be more predominantly acted as anodic type, inhibiting oxidation reactions happening on the metal surface [52]. A good agreement is also shown among the values of inhibition efficiency obtained by polarization studies and weight loss measurements.

Mechanism of Corrosion Inhibition

Aluminium metal exists in positive state in acidic medium and so expected to react with chloride ion from 0.5M HCl to form $(AlCl)^-$ [30]. MCPE inhibitor is characterized with the presence of different chemical constituents rich with O, N and S atoms, which possess lone pair of electrons. So MCPE is expected to be protonated in acidic medium. The protonated inhibitor is expected to be adsorbed on the negatively charged aluminium surface by electrostatic force of attraction [28, 30]. The adsorption phenomenon is confirmed by SEM studies shown in Fig.13. The adsorbed MCPE is expected form a thick film on the surface of aluminium and inhibit the corrosion.

Scanning Electron Microscopy

The changes of surface morphology of aluminium sample in 0.5M HCl medium in the absence and presence of MCPE inhibitor gave good results confirming the action of MCPE as a potent inhibitor. The SEM images are shown in Fig.13. The images show more pits, cavities

Table 9 : Electrochemical parameters for aluminium in 0.5M HCl at 303K for various % volumes of MCPE.

% Volume of the MCPE	i_{corr} (mA/cm²)	ßa (mV)	ßc (mV)	I.E. (%)	E_{corr}	I.E.(%) (Wt.Loss)
0	4.0309	140.45	175.11	-	-817.48	-
8	1.7755	43.85	158.06	55.95	-843.55	47.84
16	1.3100	32.78	126.27	67.50	-826.38	64.43
24	1.0225	23.55	183.48	74.63	-789.05	68.35
32	0.8510	15.92	113.77	78.88	-770.32	84.81

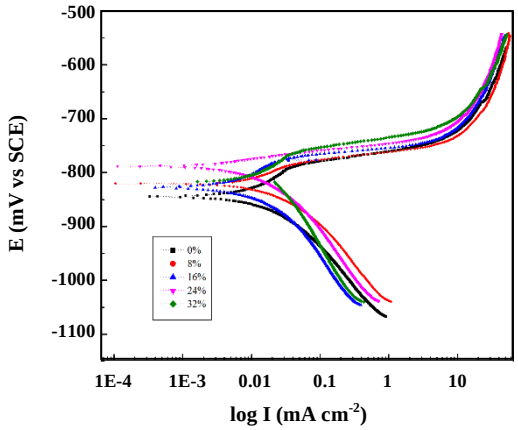

Fig. 12: Potentiodynamic polarisation curves of aluminium in 0.5 M HCl solution at 30 ^{0} C containing various % volumes of MCPE inhibitor.

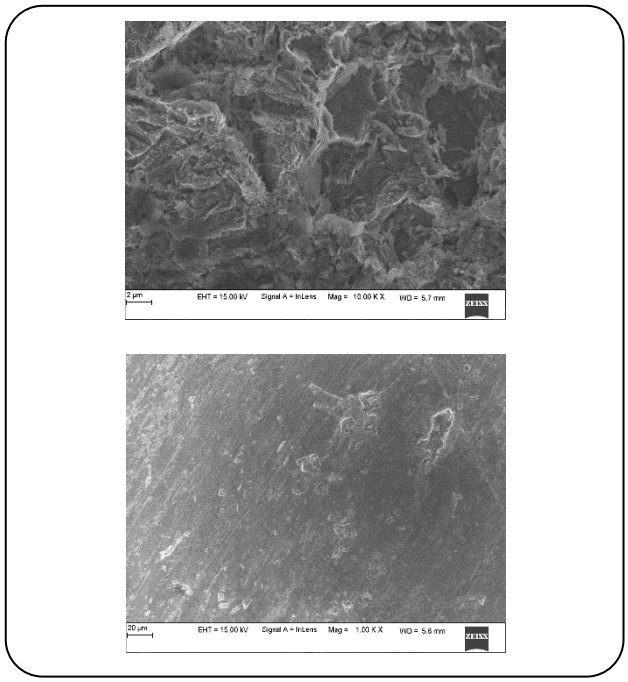

Fig. 13: SEM images of surface of aluminium after immersion for 5 hours at 303K in (a) 0.5M HCl, (b) 0.5M + 32% MCPE inhibitor.

and crevices on the surface of aluminium in the absence of MCPE in acidic medium compared to that of its presence. This confirms that the MCPE inhibitor have shown a strong adsorption on the surface of aluminium and considerably decreased the surface corrosion by covering the metal surface [53].

CONCLUSIONS

The FT-IR and GC-MS study showed the possible functional groups that involve in adsorption and the presence of most likely to be present chemical constituents in the extract indicating MCPE can act as novel green inhibitor. The thermal decomposition characteristics of the extract obtained by TGA-DSC spectrum supported GC-MS results. The corrosion tendency of aluminium in the hydrochloric acid medium found to decrease with the increase in the % volume of MCPE in all the experimentation methods adopted viz., weight loss, impedance studies and potentiodynamic polarization studies showed MCPE as a strong corrosion inhibitor. In the studied temperature range, the inhibition efficiency decreased with increase in temperature indicating that adsorption of the inhibitor on the surface of metal is of physisorption type. A decrease in the capacitance of double layer and increase in resistance due to charge transfer shown in EIS study showed MCPE as a potent inhibitor. Polarization studies demonstrated MCPE retarded both oxidation and reduction, with dominating anodic type of inhibition. Surface images of metal by SEM studies showed the mechanism of inhibition by adsorption of MCPE on to the surface of target metal.

Acknowledgements

- The authors of this paper profusely extend their gratitude towards Dr Nithyananda Shetty A, Professor, Dept of chemistry, NITK, Surathkal for their help and support.

● Authors are also grateful to DST-PURSE, Mangalore University for their timely help in providing TGA/DSC, SEM results.

Received : Sept. 24, 2019 ; Accepted : Jan. 13, 2020

REFERENCES

[1] E.McCafferty.,"Introduction to Corrosion Science", Springer Publications-Verlog, New York (2010).

[2] Nestor Perez., "Electrochemistry and Corrosion Science", Springer Pvt.,Ltd, New Delhi (2010).

[3] Zaki Ahamed., "Principles of Corrosion Engineering and Corrosion Control", Butterworth-Hineman Publications (2006).

[4] John. R. Dyer., "Applications of Absorption Spectroscopy of Organic Compounds", Prentice Hall of India, New Delhi (1989)

[5] Pretsch E.., Buhlmann P.., Badertscher M.., "Structure Determination of Organic Compounds Tables of Spectral Data" (2000)

[6] Gary D. Christian,"Analytical Chemistry", John Wiley and Sons Inc., Singapore (2004)

[7] Michael E. Brown., "Introduction to Thermal Analysis Techniques and Applications" Kluwer Academic Publishers New York, Boston, Dordrecht, London, Moscow (2001).

[8] Fifield F.W., Kealey D.,"Principles and Practice of Analytical Chemistry", Blackwell Science Ltd, London (2000)

[9] Bashir. S., Thakur. A., Lgaz. H., Chung. I.M., Kumar. A., Computational and Experimental Studies on Phenylephrine as Anti-Corrosion Substance of Mild Steel in Acidic Medium. *J. of Molecular Liquids*: 111539 (2019)

[10] Jafari H.., Danaee. I., Eskandari H.., Rashvand Ave.i M., Electrochemical and Quantum Chemical Studies of N, N'-bis(4-hydroxybenzaldehyde)-2,2-dimethylpropandiimine Schiff Base as Corrosion Inhibitor for Low Carbon Steel in HCl Solution, *J. Environment. Sci. Health*, Part A, **48**: 1628–1641 (2013).

[11] Jafari H., Danaee I., Eskandari H., Rashvand Ave.i. M., Combined Computational and Experimental Study on the Adsorption and Inhibition Effects of N_2O_2 Schiff Base on the Corrosion of API 5L Grade B Steel in 1 mol/L HCl, *J. Mater. Sci. Technol.*,**30**: 239-252 (2014).

[12] Kumar. A., Bashir. Ethambutol S.: A New and Effective Corrosion Inhibitor of Mildsteel in Acidic Medium. *Russian J. of Applied Chemistry*, **89(7)**:1158-1163(2016).

[13] Patel N. S., S. Jauhariand., Mehta G. N., Al-Deyab S. S., Warad I., Hammouti B., Mild Steel Corrosion Inhibition by Various Plant Extracts in 0.5 M Sulphuric Acid, *Int. J. Electrochem. Sci.*, **8**: 2635 - 2655 (2013)

[14] Bashir S., Sharma V., Lgaz H., Chung I.M., Singh A., Kumar. A., The Inhibition Action of Analgin on the Corrosion of Mild Steel in Acidic Medium: A Combined Theoretical and Experimental Approach, *J. of Molecular Liquids*, **263**: 454-462 (2018).

[15] Jafari H., Sayin K., Electrochemical and Theoretical Studies of Adsorption and Corrosion Inhibition of Aniline Violet Compound on Carbon Steel in Acidic Solution, *J. of the Taiwan Institute of Chemical Engineers*, **56**: 181-190 (2015).

[16] Jafari H., Danaee I., Eskandari H., RashvandAve i M., Electrochemical and Theoretical Studies of Adsorption and Corrosion Inhibition of N, N′-Bis(2-hydroxyethoxyacetophenone)-2,2-dimethyl-1,2-propanediimine on Low Carbon Steel (API 5L Grade B) in Acidic Solution, *Ind. Eng. Chem. Res.*,**52**: 6617−6632 (2013).

[17] Bashir S., Lgaz H., Chung I. M., Kumar A., Potential of Venlafaxine in the Inhibition of Mild Steel Corrosion In HCl: Insights from Experimental and Computational Studies, *Chemical Papers*, **73(9)**: 2255-2264(2019).

[18] Jafari H., Sayin K., Sulfur Containing Compounds as Corrosion Inhibitors for Mild Steel in Hydrochloric Acid Solution, *Transactions of the Indian Institute of Metals*, **69**: 805–815 (2016).

[19] David Hasson et.al, State of the Art of Friendly "Green" Scale Control Inhibitors: A Review Article, *Ind. Eng. Chem. Res.*,**50 (12)**: 7601–7607 (2011).

[20] Devarayan Kesavan., Mayakrishnan Gopiraman., Nagarajan Sulochana., Green Inhibitors for Corrosion of Metals: A Review, *Che. Sci Rev Letters* **1(1)**: 1-8(2012).

[21] Lekan Taofeek Popoola., Organic Green Corrosion Inhibitors (OGCIs): A Critical Review, *Corr. Rev*, **37(2)**: 71–102 (2019).

[22]. Popoola L.T, Grema A.S., Latinwo G.K., Gutti B., Balogun A.S., Corrosion Problems During Oil and Gas Production and Its Mitigation, *International Journal of Industrial Chemistry*, **4(1)**: 35- (2013).

[23] P.Shwethambika., J.Ishwara Bhat., *Theobroma Cocoa* Dry Bean Extract as a Potential Green Inhibitor for Mild Steel in Acidic Medium, *Iranian J. of Energy and Environment*, **10(3)**:190-199 (2019).

[24] www.powo.science.kew.org

[25] www.perfectdailygrind.com/

[26] Azizah Othman., A.I.N.A. Ilham Adenan., Antioxidant Capacity and Phenolic Content of Cocoa **B**eans, *Food Chem*,**100 (4)**:1523-1530(2007)

[27] Umoru L.E., Fawehinmi I.A., Fasasi A.Y., Investigation of the Inhibitive Influence of *Theobroma Cacao* and *Cola Acuminata Leaves* Extracts on the Corrosion of a Mild Steel in Sea Water, *J. of Applied Sciences Research*, **2(4)**: 200-204 (2006).

[28] Yuli Yetri Emriadi, Novesar Jamarun.,Gunawarman., Corrosion Inhibitor of Mild Steel by Polar Extract of *Theobroma cacao* Peels in Hydrochloric Acid Solution, *Asian J. of Chemistry* ,**27(3)**: 875-881 (2015).

[29] Raghavendra N., Ishwara Bhat J., Green Approach to inhibition of Corrosion of Aluminium in 0.5 M HCl Medium by Tender Arecanut Seed Extract: Insight from Gravimetric and Electrochemical Studies, *Springer Publication* , **42(7)**: 6351–6372 (2016).

[30] J.Ishwara Bhat., Vijaya.D.P.Alva., Corrosion Inhibition of Aluminium by 2-Chloronicotinic Acid in HCl Medium, *Indian J. of Chemical Technology* ,**16**: 228-233 (2009)

[31] www.hindalco.com

[32] P.O. Ameh., N.O.Eddy., Commiphora Pedunculata Gum as a Green Inhibitor for the Corrosion of Aluminium Alloy in 0.1 M HCl, *Res Chem Intermed*, **40**:2641–2649 (2014).

[33] hwara Bhat J., Vijaya D. P. Alva., A Study of Aluminium Corrosion Inhibition in Acid Medium by an Antiemitic Drug, *Transactions of the Indian Institute of Metals*, **64(4-5)**: 377–384 (2011).

[34] Chaithra P., Hemashree K., J. I. Bhat ., An Investigation on the Attack of Dye Species on Freshly Synthesized and Characterized Activated Carbon from Cocoa Pod, *Iranica Journal of Energy and Environment*, **7(4)**: 350-358(2016)

[35] Maxwell Adjin-Tetteh., David Dodoo Arhin., Nana Y. Asiedu., Ayman Karam., Thermochemical Conversion and Characterization of Cocoa Pod Husks A Potential Agricultural Waste from Ghana, *Ind. Crops and Products* (in press) March (2018).

[36] Evgeniya N.Ermakova., SergeyV.Sysoev., Trimethyl(phenyl)silane—a Precursor for Gas Phase Processesof SiCx:H Film Deposition: Synthesis and Characterization, *Modern Ele. Materails.*, **1**: 114-119 (2015).

[37] Rafid Hadi Hameed., Haider Mashkoor Hussein., Imad Hadi Hameed., Analysis of Bioactive Chemical Compounds of Methanolic Seed Extract of Annona cherimola (Graviolla) Using Gas Chromatography – Mass Spectrum Technique, *Indian. J. of Public Health Research & Development* ,**9**: 471-475 (2018).

[38] Adewole E., Ajiboye B., Ojo B., Ogunmodede O.T., and Oso., Characterization of Cocoa (*Theobroma cocoa*) Pod, *Int. J. of Scientific & Engineering Research*, **4(1)**: 1-5 (2013).

[39] Nurian Johar., Ishak Ahmad., Alain Dufresne., Extraction, Preparation and Characterization of Cellulose Fibres and Nanocrystals from Rice Husk, *Ind. Crops and Products*, **37(1)**: 93-99 (2012).

[40] K.Hemashree., J.Ishwara Bhat., Synthesis, Charecterization and Adsorption Behaviour of Coconut Leaf Carbon, *Res. Chem. Intermed.*, **43**:4369-4386(2017).

[41] R.Mehdaoui., A.Khelifa.., O.Aaboubi., Inhibiting Effect of Some Synthesized Surfactants from Petroleum Oils on The Corrosion of Aluminium in Hydrochloric Acid Solution, *Res. Chem. Intermed.*, **41**:705–720 (2015).

[42] Eddy N.O.., Patricia A. Ekwumemg., Paul A.P. Mamza., Ethanol Extract o Terminalia Catappa as a Green Inhibitor for te Corrosion of Mild Steel in H_2SO_4, *Green Chemistry Letters and Reviews*, **2(4)**:223-231 (2009).

[43] E.E.Oguzie., Corrosion Inhibition of Aluminium in Acidic and Alkaline Media by *Sansevieria trifasciata* Extract, *Corr. Science*, **49(3)**: 1527-1539 (2007).

[44] Popova., A., Christov, M., Evaluation of Impedance Measurements on Mild Steel Corrosion in Acid Media in the Presence of Heterocyclic Compounds, *Corr. Science*, **48(10)**: 3208-3232 (2006).

[45] Aytac., Cu(II), Co(II) and Ni(II) Complexes of –Br and $–OCH_2CH_3$ Substituted Schiff Bases as Corrosion Inhibitors for Aluminium in Acidic Media, *J. Mater. Sci.*, **45**: 6812–6818(2010).

[46] Ekanem U.F., Umoren S.A., Udousoro I.I., Udoh. A.P., Inhibition of Mild Steel Corrosion in HCl Using Pineapple Leaves (Ananas comosus L.) Extract, *Springer Science+Business Media, LLC,* **45(20)**: 5558-5566 (2010).

[47] Jafari, Hojat., Mohsenifar, Farhad., Sayin, Koray., Effect of Alkyl Chain Length on Adsorption Behavior and Corrosion Inhibition of Imidazoline Inhibitors, *Iran. J. Chem. Chem. Eng.*, **37(5)**: 85-103(2018).

[48] Jafari H., Akbarzade K., Effect of Concentration and Temperature on Carbon Steel Corrosion Inhibition, *J.of Bio-and Tribo Corrosion*,**3**:8–14 (2017).

[49] Mohsenifar F., Jafari H., Sayin K., Investigation of Thermodynamic Parameters For Steel Corrosion in Acidic Solution in the Presence of N, N′-bis (phloroacetophenone)-1, 2 propanediamine, *J. of Bio-and Tribo-Corrosion*,**2**: 1 (2016).

[50] Bentiss F., Traisnel M., Lagrenee M., The Substituted 1,3,4-Oxadiazoles: A New Class of Corrosion Inhibitors of Mild Steel in Acidic Media, *Corr. Science*, **42(1)**:127-146 (2000).

[51] Namrata Chaubey., Vinod Kumar Singh., Savita., M. A. Quraishi., Eno E. Ebenso., Corrosion Inhibition of Aluminium Alloy in Alkaline Media by Neolamarkia Cadamba Bark Extract as a Green Inhibitor, *Int. J. Electrochem. Sci.*, **10**: 504-518 (2015).

[52] S. Gudić., L. Vrsalović. , M. Kliškić., I. Jerković., A. Radonić. , M. Zekić., Corrosion Inhibition of AA 5052 Aluminium Alloy in NaCl Solution by Different Types of Honey, *Int. J. Electrochem. Sci*., **11**: 998-1011 (2016).

[53] PDR Kumari., J Nayak., AN Shetty., Corrosion Behavior of 6061/Al-15 vol. pct. SiC (p) Composite and the Base Alloy in Sodium Hydroxide Solution, *Arabian Journal of Chemistry*, **9**: 1144-1154 (2016).